

Radon transforms and multiple attenuation of White Rose data

Zhihong (Nancy) Cao and John C. Bancroft

ABSTRACT

One of the current hot topics in exploration geophysics is multiple attenuation. Various Radon transform methods have received attention in this research area. This report describes the analysis and testing of several formulations of the Radon transform technique including the least-squares solution, the frequency domain high resolution solution and the $x-t$ domain high resolution Radon transform, which are commonly used in industry. After testing with synthetic seismic data, multiple elimination was performed on White Rose field data by applying the high resolution Radon transform.

INTRODUCTION

A long standing problem of exploration geophysics, multiple reflections has been one of the most interesting research topics. Multiple attenuation can be achieved by the Radon transform, using velocity discrimination of multiple reflections with respect to primary reflections. The Radon transform is defined as an integration of data along certain stacking paths (Radon, 1917). For example, linear paths, parabolic paths and hyperbolic paths are most commonly used in exploration geophysics. The Radon transform experiences a smearing problem when applied to seismic data, due to limited offset range of seismic gathers and energy smearing along offsets, especially at near offsets, which decreases the resolution and efficiency of the Radon transforms. As a consequence, multiple reflections are not well separated from primaries when their velocity differences are not dramatic.

The Radon transform is not an orthogonal algorithm. Therefore, data loss can not be avoided when the forward and inverse Radon transforms are applied to data (Trad et al, 2003). The research objectives for Radon multiple attenuation methods are to minimize the data loss and improve the resolution in the Radon domain.

The time domain least-squares solution and a high resolution stochastic inversion method were proposed by Thorson and Claerbout (1985). A sparse solution of the Radon transform is achieved by the stochastic inversion method in both τ and q directions. However, implementation of these methods in the time domain is very time consuming and expensive, which is why these methods are not popular with industry. A faster least-squares solution applied over NMO-corrected CMP gathers in the frequency domain was then suggested by Hampson (1986). This method can also be performed over t^2 -stretched CMP gathers (Yilmaz, 1989). However working on t^2 -stretched datasets is much more expensive than on NMO-corrected datasets due to much larger range along the q axis. Sacchi and Ulrych (1995) proposed the high resolution Radon transform in the frequency domain, which provides a sparse solution along the q axis. Cary (1998) pointed out the superiority of the stochastic inversion method due to its characteristic sparseness in both the time and q directions.

Compared to the conventional Radon transform, a time domain semblance-weighted Gauss-Seidel method proposed by Bradshaw and Ng (1987) and Yilmaz and Taner (1994) provides a relatively more focused Radon panel. Ng and Perz (2004) then suggested an x - t domain high resolution Radon solution. This approach is an improved solution of the time domain semblance-weighted Gauss-Seidel method. The computation of this Radon solution is achieved by an intelligent choice of the q sequence, which is estimated from the results of the initial semblance-weighted Gauss-Seidel method.

The conventional least-squares solution, the high resolution frequency domain Radon method, and the high resolution x - t domain method are analyzed in the next section of this paper.

ANALYSIS OF THE RADON SOLUTIONS WITH SYNTHETIC DATA

Introduction to Radon solutions

The discrete form of the conventional Radon transform with a parabolic integration path is defined as follows:

$$u(\tau, q) = \sum_h d(t = \tau + qh^2, h), \quad (1)$$

where d stands for a CMP or shot gather or the so called the data space, u represents the Radon panel obtained by the forward Radon transform and is also called the model space, t is the two-way time axis in the x - t domain, h is the half offset, τ is the intercept time, and q is the slope of the stacking path, which is defined by $t = \tau + qh^2$. The matrix form of the forward and inverse transforms can be written as:

$$\mathbf{u} = \mathbf{L}^T \mathbf{d}, \quad (2)$$

$$\mathbf{d} = \mathbf{L} \mathbf{u}. \quad (3)$$

However, \mathbf{L}^T and \mathbf{L} are not mutually inverse to each other, where \mathbf{T} donates transpose. Equation (1) and (2) provides only a low resolution Radon panel. In the least-squares solution suggested by Thorson and Claerbout (1985), the inverse format of \mathbf{L} is defined as approximately:

$$\mathbf{L}^{-1} \approx (\mathbf{L}^T \mathbf{L} + \mu \mathbf{I})^{-1} \mathbf{L}^T, \quad (4)$$

where $\mu \mathbf{I}$ is a perturbing factor ensuring a stable inverse of the operator $\mathbf{L}^T \mathbf{L}$. Then the least-squares format of the forward Radon transform becomes:

$$\mathbf{u} = (\mathbf{L}^T \mathbf{L} + \mu \mathbf{I})^{-1} \mathbf{L}^T \mathbf{d}, \quad (5)$$

where μ is a damping factor to insure stable inversion. A stochastic inverse solution was also discussed by Thorson and Claerbout (1985), where \mathbf{D} , the ratio of noise variance to signal variance in the model space, replaces $\mu \mathbf{I}$ to achieve a nonlinear sparseness measure of the model space in both time and q directions. However, the matrix \mathbf{L} is a very large matrix and it is time consuming to invert the matrix $\mathbf{L}^T \mathbf{L}$. In order to avoid this tedious computation, Hampson (1986) defined the parabolic Radon transform over NMO-

corrected gathers. The invariant moveouts along parabolic stacking paths in time direction makes it possible to implement the algorithm in the frequency domain, which is dramatically faster than the time domain algorithm. A sparse Radon transform solution along the q axis in the frequency domain by means of Bayes rule was proposed by Sacchi and Ulrych (1995), which is the so called high resolution Radon transform:

$$\mathbf{u} = (\mathbf{L}^T \mathbf{L} + \mathbf{D})^{-1} \mathbf{L}^T \mathbf{d}, \quad (6)$$

where * donates complex conjugate. The matrix \mathbf{D} has the form as:

$$\mathbf{D} = \frac{\mu \mathbf{I}}{b + |u_i|^2}, \quad (7)$$

and where u_i is initially determined by the conventional least-squares solution defined by equation (5) implemented in frequency domain, and b is a small number to guarantee the existence of \mathbf{D} . The elements of the matrix \mathbf{D} are basically inversely proportional to the ‘energy’ of the model estimated from the previous preliminary transform. The matrix \mathbf{D} is computed in each iteration of the high-resolution transform.

The semblance-weighted Gauss-Seidel Radon method was introduced by Bradshaw and Ng (1987) and Ng and Perz (2004). The semblance of a CMP gather in a parabolic shape is defined as:

$$S(\tau, q) = \frac{\sum_l \left(\sum_h d(t = \tau + qh^2, h) \right)}{N_h \sum_l \sum_h d^2(t = \tau + qh^2, h)}, \quad (8)$$

where S is the semblance; l is a window size and is usually a wavelet length; N_h is the number of traces involved in the semblance calculation. Semblance has an important property that its value is independent of the amplitudes of the input dataset and it ranges from 0-to-1 as an indication of poorest-to-best fit of the proposed trajectory respectively (Bradshaw and Ng, 1987). Semblance is a coherency measurement of events. Weighting the forward Radon transform with semblance can enhance energy cluster along those trajectories which fit seismic events well in the seismic dataset and weaken energy along those trajectories which badly fit seismic events. Applied in the Gauss-Seidel sense which means data transformed into the Radon panel will be removed from the input data space, the semblance-weighted Radon approach produces moderately high resolution results. The weighted Radon transform for the parabolic trajectory is then defined as follows:

$$u(\tau, q) = S(\tau, q) \sum_h d(t = \tau + qh^2, h). \quad (9)$$

Inspired by the idea of the frequency domain high resolution Radon transform, a high resolution method in the x - t domain based on the semblance-weighted Gauss-Seidel method was implemented by Ng and Perz (2004). After the first iteration of semblance-weighted Radon calculation, an estimation of the model space is measured along q -axis.

In the next iteration of calculation, the transform is first performed along these q traces, which contain the most model energy, and at the same time the transformed energy is again removed from the data space. Sparseness on the q -axis is achieved during this process and sparseness on the τ -axis is achieved by application of semblance.

Synthetic data examination

A synthetic NMO-corrected CMP gather shown in Figure 1 contains offsets from 0 to 2500 m, and the trace interval is 20 m. Two primaries, Pa and Pb with constant amplitudes across the offsets, which are flat after NMO correction, are located at 0.3 s and 0.57 s respectively. One of the five parabolic multiple events, Ma, has the same travel time at zero offset, and its moveout at the far offset is 20 ms. Notice that Ma is very close to Pa and they are difficult to differentiate. Even at the far offsets, the two events are partially mixed together. Event Mb, with a travel time of 0.5 s at zero offset and moveout of 70 ms at the far offset, overlaps the primary Pb at far offsets; Event Mc is located at 0.7 s at zero offset. Event Md, with a vertical travel time of 1.02 s and a moveout of 120 ms at the far offset, has variable amplitudes at the near offsets; and Me, with a vertical travel time of 1.3 s and a moveout of 150 ms at the far offset, shows variable amplitude effects at far offsets.

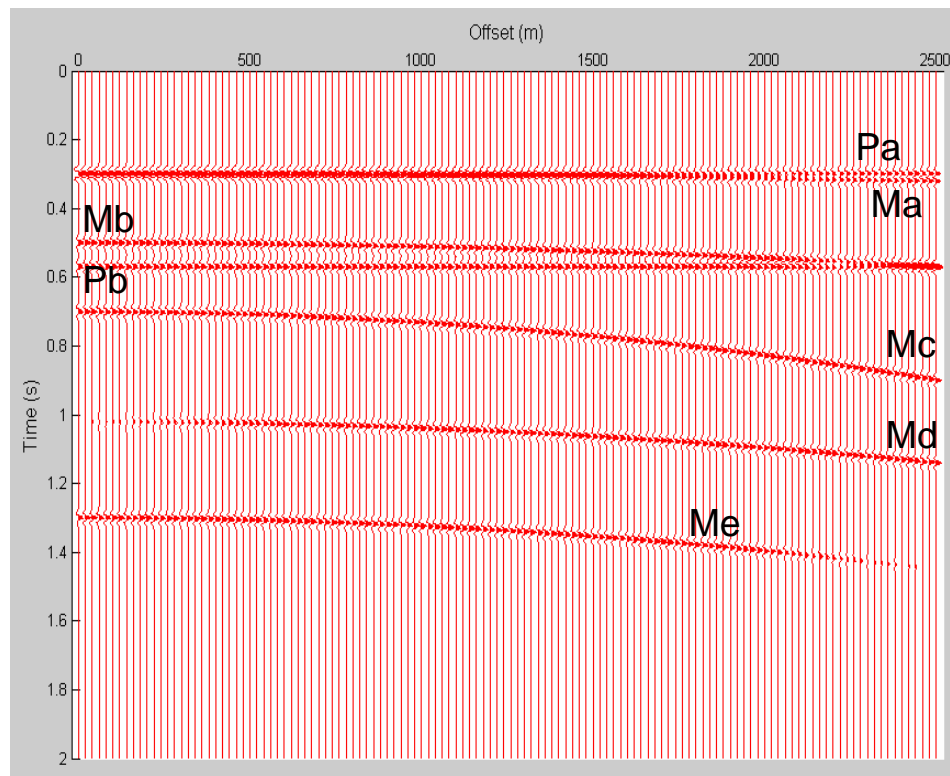


FIG. 1. The synthetic NMO-corrected CMP gather. All of plots of this gather in x - t domain are scaled to this plot.

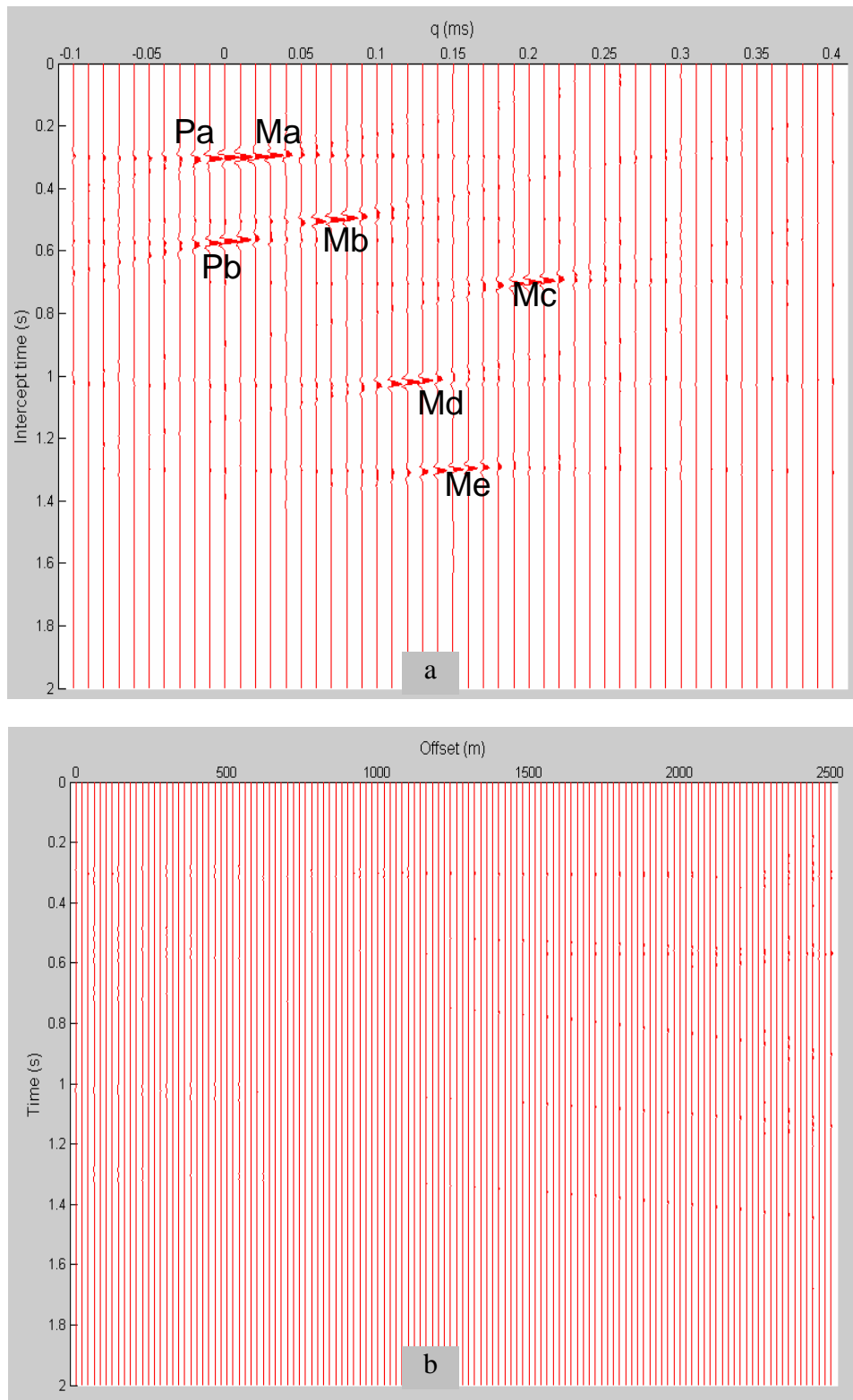


FIG. 2(a). The Radon panel computed by the conventional least-squares solution; (b) the difference between the reconstructed gather and the original gather.

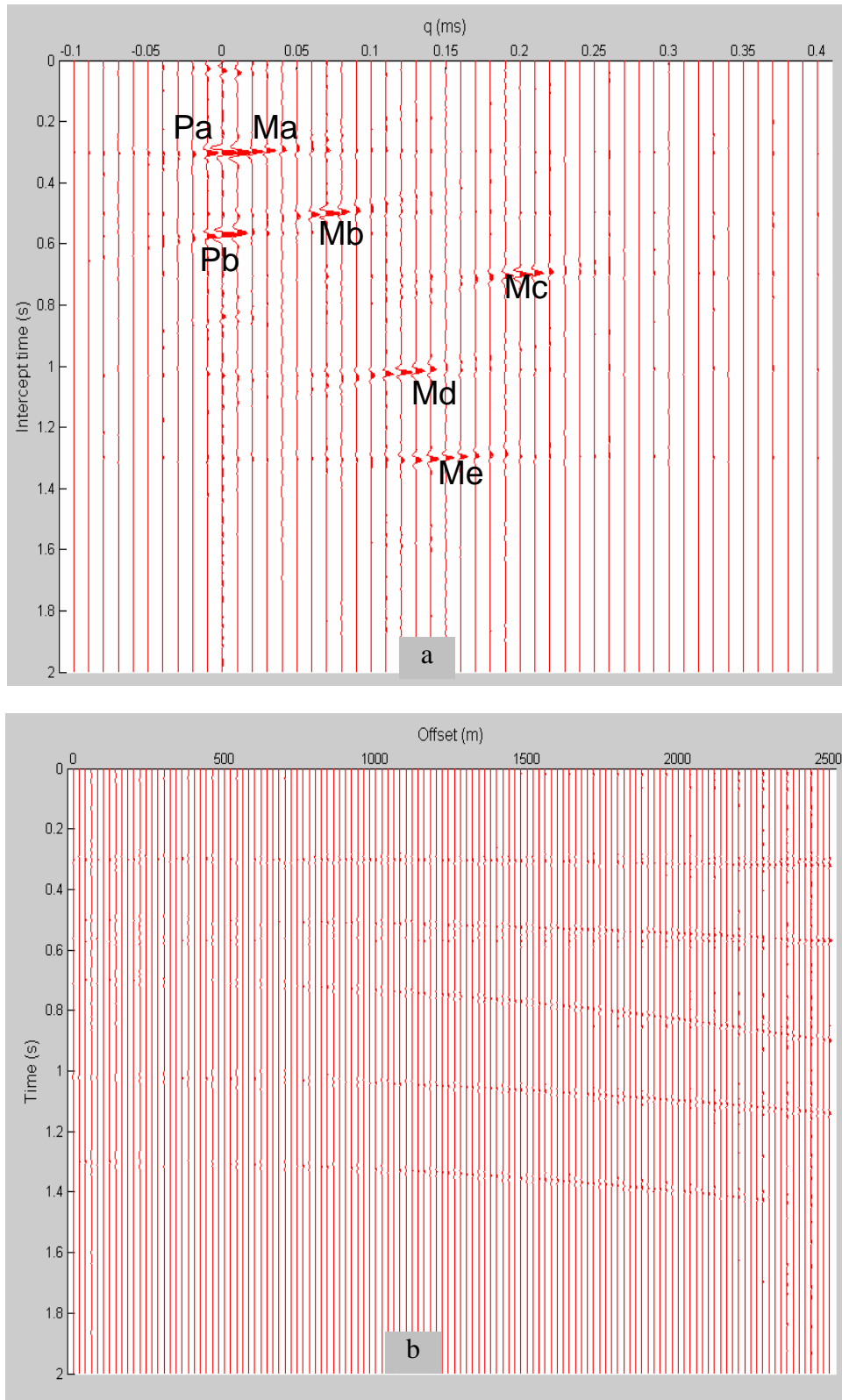


FIG. 3(a). The Radon panel computed by Sacchi and Ulrych algorithm; (b) the difference between the reconstructed gather and the original gather.

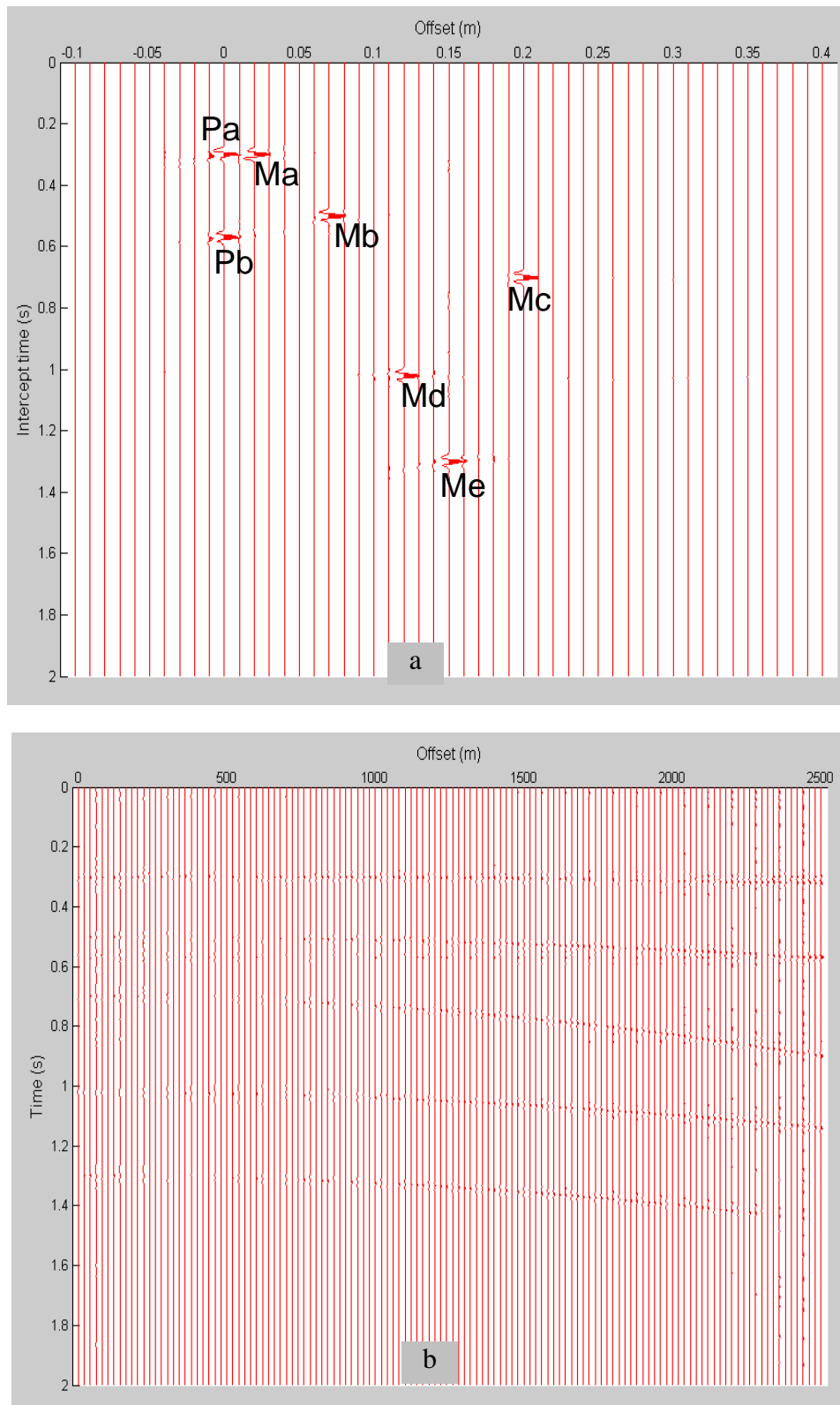


FIG. 4(a). The Radon panel computed by Ng and Perz algorithm; (b) the difference between the reconstructed gather and the original gather.

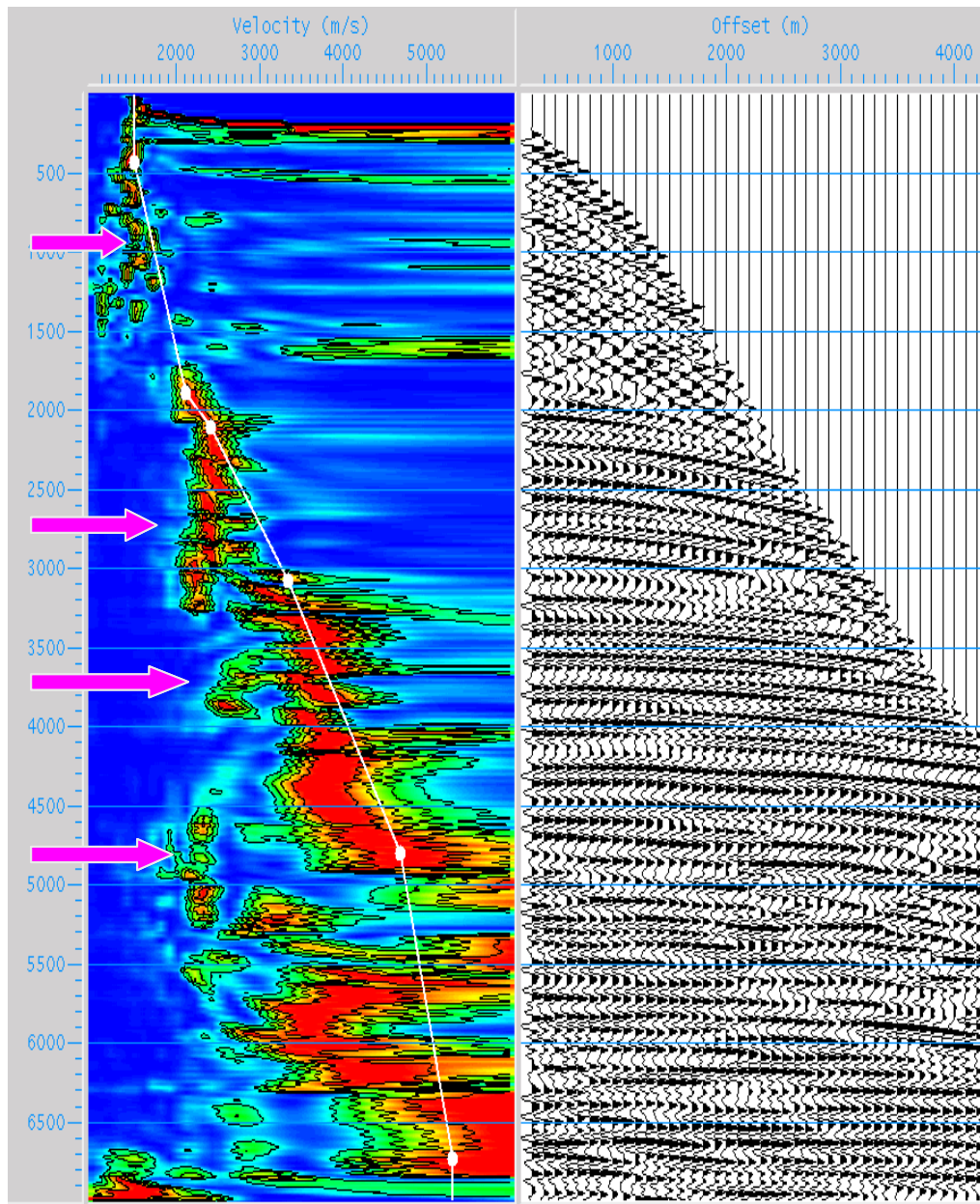


FIG. 5. A CMP gather from offshore White Rose and its semblance plot.

For each of the three methods: the conventional least-squares solution (Hampson, 1986; Yilmaz, 1989), the iterative frequency domain high resolution method (Sacchi and Ulrych, 1995) and the $x-t$ domain high resolution method (Ng and Perz, 2004), the Radon panel and the difference gather between the reconstructed and original gather in Figure 1 are shown in Figures 2, 3, and 4, respectively. All of these three methods provide relatively good reconstruction judging from the residual gathers. A relatively smeared Radon panel is provided by the least-squares solution as shown in Figure 2 (a). Specifically, events Pa and Ma can't be separated from each other. The Radon panel in Figure 3 (a), done by the frequency domain high resolution method, is more focused and less smeared compared to Figure 2 (a). However, events Pa and Ma are still hardly resolved in the Radon panel. A clear image shown in Figure 4 (a) is calculated by the $x-t$

domain high resolution method. Event Ma is apparently separated from the primary Pa. All of these three methods are able to preserve the AVO effects in the $x-t$ domain, such as events Md and Me.

MULTIPLE ATTENUATION OF WHITE ROSE DATA

A CMP gather and its semblance plot from marine streamer data from the White Rose prospect, which is located on the east coast of Canada, is shown in Figure 5. Strong water column multiples and peg-leg multiples can be recognized from both the gather and its semblance plot as indicated by the pink arrows. Primaries are badly contaminated by these multiples. It's difficult to do velocity analysis in this area.

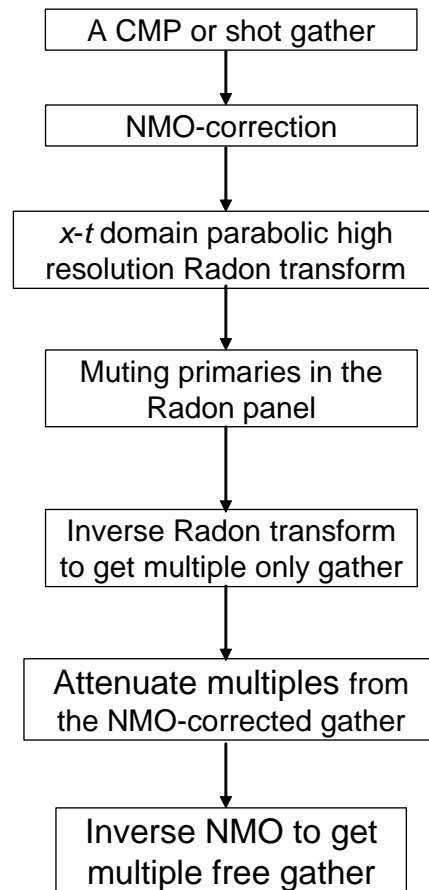


FIG. 6. Workflow for multiple attenuation.

A multiple attenuation workflow shown in Figure 6 was applied to this gather using the parabolic $x-t$ domain high resolution Radon transform. Note that the gather was NMO-corrected before the application of the Radon transform. The Radon panel is displayed in Figure 7. Since the input data are NMO-corrected, which implies that primaries are flattened and their slopes, q , are zero, primary energy is clustered along $q=0$ as indicated on the figure. The $x-t$ domain gather containing only multiple reflections was obtained by muting primaries and inverse Radon transforming the residual data which are supposed to be multiple reflections. The multiple gather, after inverse NMO-correction, and its semblance plot are shown in Figure 8. Compared to the semblance plot in Figure

5, the clarity of velocity information of multiple reflections is apparent on this semblance plot. A multiple-free gather was then obtained by subtracting the multiple gather in Figure 8 from the original gather. After inverse NMO-correction, this multiple free gather and its semblance plot are shown in Figure 9. Dramatically different from Figure 5, velocity analysis can be performed more easily on this semblance plot.

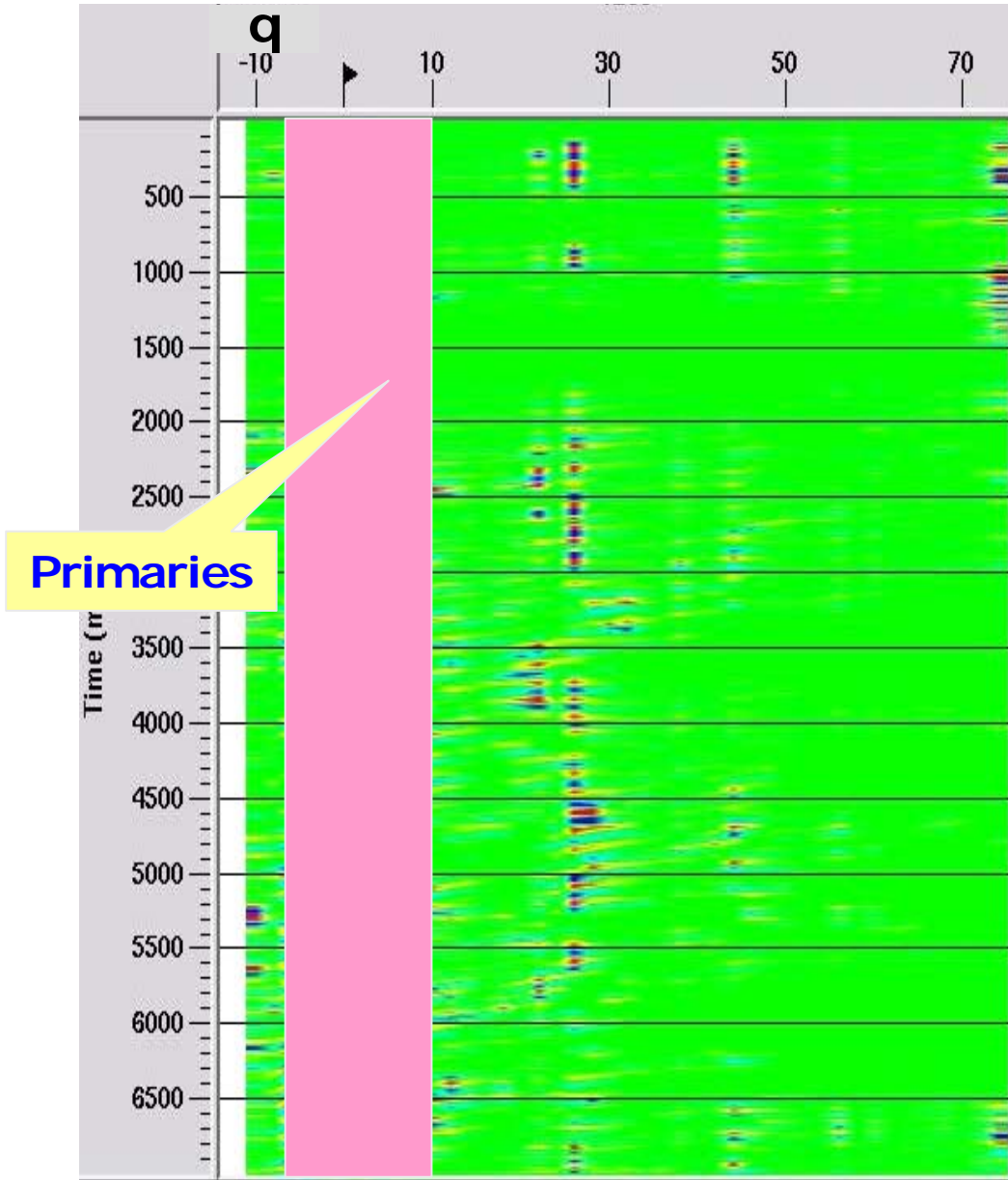


FIG. 7. The Radon panel of the NMO-corrected gather.

CONCLUSIONS

Three Radon solutions are analyzed and tested with a synthetic dataset in this paper. The results show that all of these three methods can satisfactorily reconstruct the input data. A relatively low resolution Radon panel was obtained using the least-squares solution. A more focused Radon panel was provided by the frequency domain high resolution Radon transform. The $x-t$ domain high resolution method yielded an especially impressive Radon transform.

Contamination by multiple reflections makes velocity analysis a very difficult job in the White Rose area. The $x-t$ domain high resolution method was applied to a CMP gather from this area to attenuate multiple reflections. The results are very impressive. After multiple attenuation, the velocity trend is very clearly shown on the semblance plot.

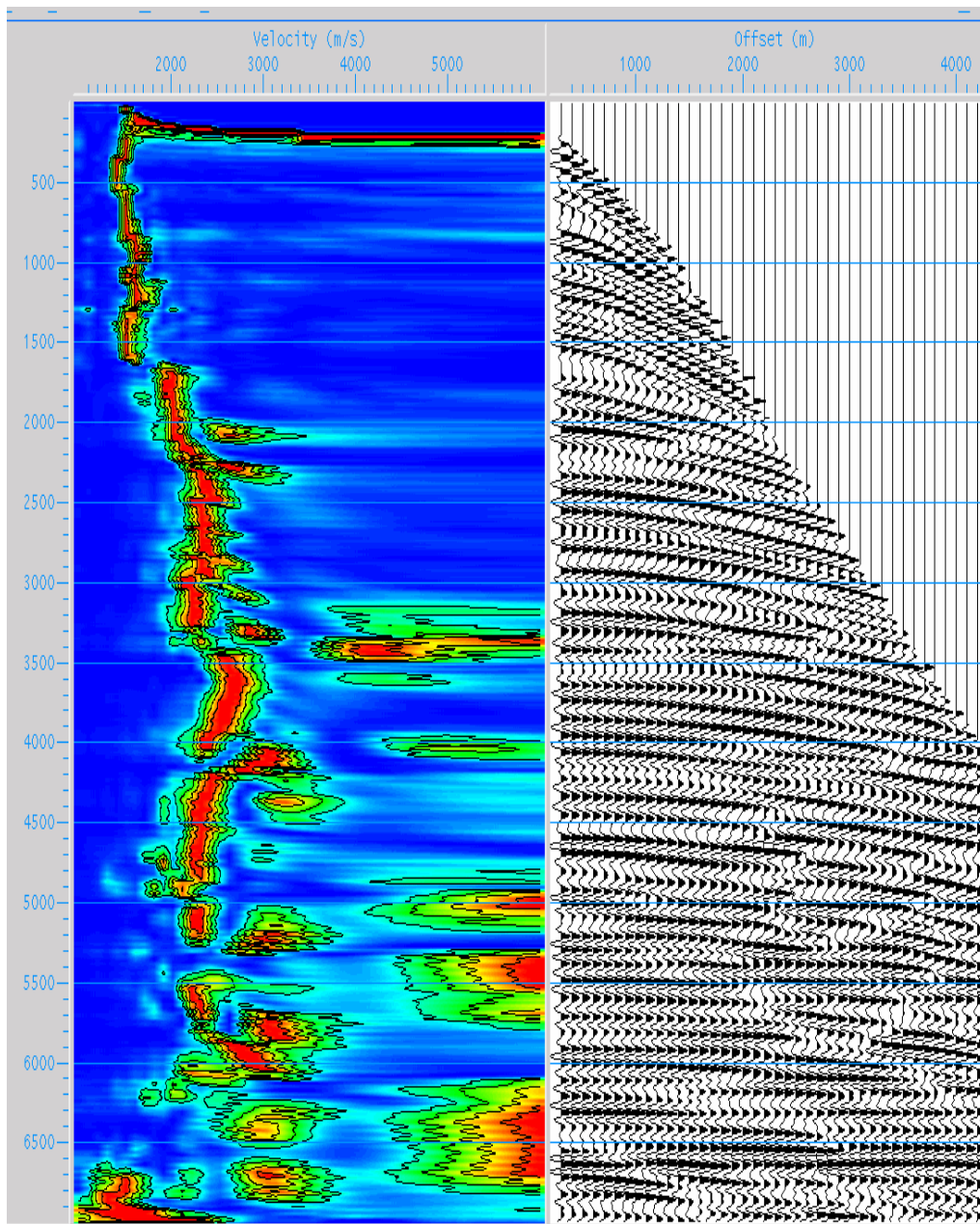


FIG. 8. The estimated multiple reflections and its semblance plot.

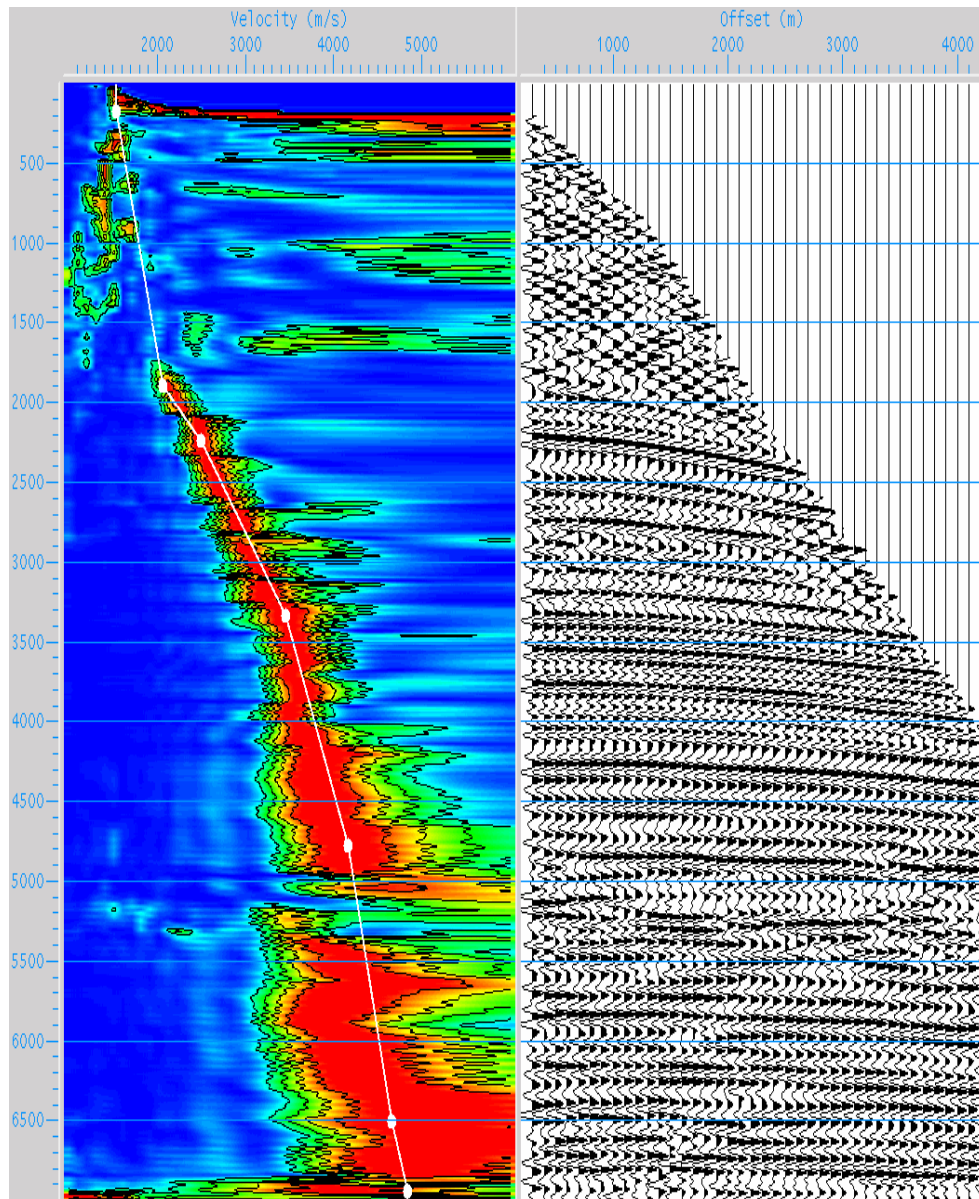


FIG. 9. After multiple removal, the CMP gather and its semblance plot.

ACKNOWLEDGEMENTS

Thanks to John Bancroft for supervising my research and study. Thanks to Mark Ng for personal discussion about the x - t domain high resolution Radon transform. Thanks are also given to Peter Cary and Mauricio D. Sacchi for discussion. Through my research, CREWES staffs have been providing effective help to me. I really appreciate it. I also give my thanks to the CREWES Project and its sponsors, University of Calgary, CSEG and SEG for support of my study.

REFERENCES

- Bradshaw, A. and Ng, M., 1987, Multiple attenuation by parabolic stack Radon transform: Geo-X Systems internal paper.
- Cary, P., 1998, The simplest discrete Radon transform: Presented at the 68th Ann. Internat. Mtg., Soc. Expl. Geophys., Expanded Abstracts, 1999-2002.
- Trad, D., Ulrych, T. and Sacchi, M. 2003, Latest views of the sparse Radon transform: *Geophysics*, **68**, 386-399.
- Hampson, D., 1986, Inverse velocity stacking for multiple elimination: *J. Can. Soc. Expl. Geophys.*, **22**, 44-55.
- Ng, M., and Perz, M., 2004, High resolution Radon transform in the t-x domain using “intelligent” prioritization of the Gauss-Seidel estimation sequence: Presented at the 74th Ann. Internat. Mtg. Soc. Expl. Geophys., Expanded Abstracts, 2160-2163.
- Sacchi, M. D., and Ulrych, T. J., 1995, High-resolution velocity gathers and offset space reconstruction: *Geophysics*, **60**, 1169-1177.
- Thorson, J. R., and Claerbout, J. F., 1985, Velocity-stack and slant-stack stochastic inversion: *Geophysics*, **50**, 2727-2741.
- Yilmaz, Ö., 1989, Velocity-stack processing: *Geophys. Prosp.*, **37**, 357-382.
- Yilmaz, Ö. and Taner, M. T., 1994, Discrete plane-wave decomposition by least-mean-square-error method: *Geophysics*, **59**, 973-982.